

Enhanced Magnetolectric Coupling in Layered Structure of Piezoelectric Bimorph and Metallic Alloy

V.M. PETROV,^{1,2} M.I. BICHURIN,¹ K.V. LAVRENTYEVA,¹
and V.S. LEONTIEV¹

1.—Institute of Electronic and Information Systems, Novgorod State University, 41 B.S.-Peterburgskaya Street, 173003 Veliky Novgorod, Russia. 2.—e-mail: vladimir.petrov@novsu.ru

We have investigated the enhanced magnetolectric (ME) coupling in a layered structure of piezoelectric bimorph and magnetostrictive metallic alloy. The observed ME coefficient in the piezoelectric bimorph-based structure was found to be two times higher than in the traditional piezoelectric/magnetostrictive bilayer. The observed enhancement in ME coupling strength is related to equal signs of induced voltage in both lead zirconate titanate layers with opposite poling directions due to the flexural deformations. The piezoelectric bimorph-based structure has promising potential for sensor and technological applications.

Key words: Magnetolectric coupling, piezoelectric bimorph, magnetostrictive material, composite materials

INTRODUCTION

A multiferroic with enabled coupling between magnetic and ferroelectric ordering that occur simultaneously is a magnetolectric (ME).^{1–4} The strain of the magnetostrictive phase in an applied magnetic field, H , is transferred to the piezoelectric phase, resulting in an electric polarization, P , due to piezoelectric coupling. The ME effect can be described by $P = \alpha H$, where α is the ME susceptibility. The bending vibrations of functionally graded ferroelectric–ferromagnetic bilayers results in an increase in ME coupling strength when the grading axis is perpendicular to the sample plane.⁵ The graded composites that have been discussed so far include layered structures based on piezoelectric barium titanate, lead zirconate titanate (PZT), lead magnesium niobate-lead titanate (PMN-PT) and magnetostrictive ferrites, manganites, metals, and alloys.^{2,3,6,7} Enhanced ME effects at low frequencies and at electromechanical resonance (EMR) have been reported for these compositions. These findings facilitate the real-world application of ME materials.

Ferroids with compositional grading show a number of novel effects such as built-in fields, vertically shifted hysteresis loop, spontaneous deformation, strong response to applied fields, and permittivity with high tunability.⁸ Theoretical models of graded ferroids enable the prediction of electro-magneto-elastic behaviors and the estimating of the effects of an external bending and twisting stress.⁹ Modeling the applied force-induced response of a graded piezoelectric-piezomagnetic composite was reported recently.¹⁰

Based on the magnetic susceptibility measurements, a built-in magnetization was obtained in graded Ni-Zn ferrite and barium hexaferrite.¹¹ Assuming the magnetization to be spatially dependent resulted in an estimate of internal magnetic field that is in accordance with the data.

We report in this work ME coefficients of compositionally graded structures based on piezoelectric PZT bimorph and magnetostrictive Metglas. Two PZT layers of piezoelectric bimorph were polarized in opposite directions and enabled us to observe the ME coupling due to flexural deformations. The observed ME coefficients in the piezoelectric bimorph-based structure was found to be 2 times higher than in the traditional structure of PZT and Metglas.

EXPERIMENTAL

We have prepared series of samples with different PZT volume fractions. Laminates of PZT–Metglas were made by bonding a 1 cm × 0.5 cm × 0.34 cm PZT and 30- μ m-thick Metglas (AMAG 492; OJSC MSTATOR, Russia) of similar lateral dimensions (Fig. 1). For greater thicknesses of Metglas, it was necessary to bond the required number of Metglas layers with 2- μ m-thick epoxy. The PZT with silver electrodes was initially poled in an electric field and was then bonded to Metglas with the epoxy. For ME characterization, measurements were made by subjecting the sample to a bias magnetic field, H , generated by an electromagnet and ac magnetic field $H_1 = 1$ Oe produced by a pair of Helmholtz coils. With the sample plane defined as (1,2), the magnetic fields were applied parallel to the length of the sample plane, along direction-1. The induced ac electric field, E_3 , and voltage, U , were measured across the thickness of the PZT through a lock-in-amplifier. The ME voltage coefficient, $\alpha_{E31} = E_{3AV}/H_1 = U/t H_1$, with E_{3AV} and t denoting the average electric field induced across the structure and the total thickness of the sample, respectively, was measured as a function of H and PZT volume fraction, v , at a constant frequency of 1 kHz.

THEORETICAL MODELING

Next, we modelled the ME interactions in a layered structure of the piezoelectric bimorph and the magnetostrictive phase consisting of several Metglas layers. The piezoelectric phase is supposed to consist of two layers, with the upper layer polarized in the opposite direction relative to the bottom layer. The sample is considered as a thin plate with thickness, t , that is assumed to be small compared to the width, w . In turn, w is supposed to be small in comparison with the length, L . The poling direction of the piezoelectric layer and the sample length are along the thickness directions, the Z - and X -axes, respectively. The applied dc bias and ac magnetic fields are parallel to the X -axis. At

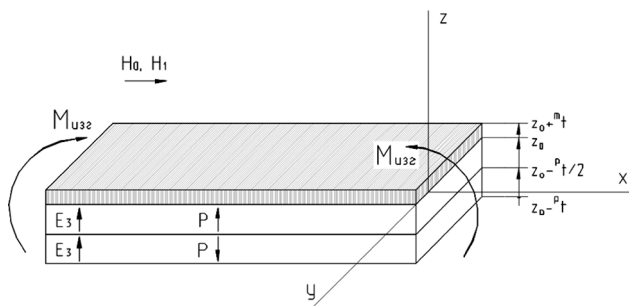


Fig. 1. The layered structure of Metglas and bimorph PZT. The sample with length L is located in the XOY plane, and the Z -axis is directed along the sample thickness. Bias field H_0 and an ac magnetic field H are applied along the X -axis. The polarization vector of the piezoelectric layers and alternating electric field, E , are directed perpendicular to the sample plane. A non-zero rotating moment, M , causes the sample flexure.

the specified conditions, only the X -components of stress can be assumed to be non-zero. The magnetically produced deformation of the magnetostrictive layer is restricted by the piezoelectric layer. The X -components of forces in the layers give rise to a bending moment with respect to the Y -axis because the forces are not applied centrally due to the asymmetry of the sample. As a result, a flexural deformation and a curvature appear. To take into account the flexural deformations, we consider the longitudinal axial strains of each layer as functions of the vertical coordinate, and these functions are assumed to be linear.

The analysis described here is based on the following equations for the strain, electric displacement and magnetic field of piezoelectric and magnetostrictive layers:

$$\begin{aligned} {}^{p1}S_1 &= {}^p s_{11} {}^{p1}T_1 + {}^p d_{31} {}^{p1}E_3; \\ {}^{p1}D_3 &= {}^p d_{31} {}^{p1}T_1 + {}^p \epsilon_{33} {}^{p1}E_3; \\ {}^{p2}S_1 &= {}^p s_{11} {}^{p2}T_1 - {}^p d_{31} {}^{p2}E_3; \\ {}^{p2}D_3 &= -{}^p d_{31} {}^{p2}T_1 + {}^p \epsilon_{33} {}^{p2}E_3; \\ {}^m S_1 &= {}^m s_{11} {}^m T_1 + {}^m g_{11} {}^m B_1; \\ {}^m H_1 &= -{}^m g_{11} {}^m T_1 + 1/{}^m \mu_{11} {}^m B_1; \end{aligned} \quad (1)$$

where S_1 and T_1 are strain and stress tensor components, E_3 and D_3 are the vector components of the electric field and electric displacement, H_1 and B_1 are the vector components of magnetic field and magnetic induction, d_{31} and g_{11} are piezoelectric and piezomagnetic, ${}^p s_{11}$ and ${}^m s_{11}$, compliance coefficients at constant electric field and constant magnetic induction, ϵ_{33} is the permittivity matrix and μ_{11} is the permeability matrix. The superscripts $p1$, $p2$, and m correspond to two piezoelectric and ferromagnetic layers, respectively. We assume the symmetry of the piezoelectric and magnetic phases to correspondingly be ∞m and cubic. In this case, the theoretical modeling is similar to recent studies on ME coupling in a bilayer of compositionally graded components.⁵ To adapt that model to this work, we assumed the longitudinal axial strains of each layer to be linear functions of the vertical coordinate, z_i , to take into account the cylindrical bending of the trilayer:¹² ${}^{p1}S_1 = {}^{p1}S_{10} + z_{p1}/R$; ${}^{p2}S_1 = {}^{p2}S_{10} + z_{p2}/R$; ${}^m S_1 = {}^m S_{10} + z_m/R$, where ${}^i S_{10}$ are the centroidal strains along the X -axis at $z_i = 0$, R is the radius of curvature and z_i is measured relative to the centroidal plane of the i -layer. It can be shown that centroidal strains obey the following conditions: ${}^{p2}S_{10} - {}^{p1}S_{10} = h_2/R$, ${}^m S_{10} - {}^{p1}S_{10} = h_1/R$, where $h_1 = ({}^{p1}t + {}^m t)/2$ and $h_2 = ({}^{p1}t + {}^{p2}t)/2$ are the distances between the centroidal planes of the first piezoelectric and magnetic layers and between that of two piezoelectric layers, while ${}^{p1}t$, ${}^{p2}t$, and ${}^m t$ are thicknesses of the three layers.

The axial forces in the three layers must add up to zero and the rotating moments of the axial forces in

the three layers must be counteracted by the resultant bending moments, mM_1 , ${}^{p1}M_1$ and ${}^{p2}M_1$, induced in the piezoelectric and two piezomagnetic layers to preserve force and moment equilibrium,

$${}^{p1}F_1 + {}^{p2}F_1 + {}^mF_1 = 0, \quad (2)$$

$${}^{p1}F_1h_1 + {}^{p2}F_1(h_1 + h_2) = {}^mM_1 + {}^{p1}M_1 + {}^{p2}M_1, \quad (3)$$

where ${}^iF_1 = \int_{-i/2}^{i/2} {}^iT_1 dz_1$, ${}^iM_1 = \int_{-i/2}^{i/2} z_i^i T_1 dz_i$,

Equations 2 and 3 enable the finding of the stress components, taking into account Eq. 1. Substituting the value of stress into an open electric circuit condition and assuming the equal thickness of the PZT layers results in an analytical expression for the ME voltage coefficient: $\alpha_{E31} =$

$$-\frac{p d_{31}}{t H_1 p \epsilon_{33}} \left(\int_{-p t_1/2}^{p t_1/2} ({}^{p1}T_1 + {}^{p2}T_1) dz \right) \text{ where } H_1 \text{ is the}$$

applied ac magnetic field. Assuming the electromechanical coupling coefficient squared to be small compared to unity enables us to obtain the expression for the ME voltage coefficient in an explicit form:

$$\alpha_{E31} = \frac{3^m q_{11} m s_{11} (1-v) v^{3p} d_{31}}{2\{(m s_{11} - p s_{11})v[(m s_{11} - p s_{11})v^3 + 4^p s_{11}(v^2 + 1) - 6^p s_{11}v] + p s_{11}^2\} p \epsilon_{33}} \quad (4)$$

where the piezoelectric volume fraction is defined as $v = ({}^{p1}t + {}^{p2}t)/t$.

One can see from Eq. 4 that the ME voltage coefficient is substantially determined by the piezoelectric coefficients of the piezoelectric phases and the piezomagnetic coefficient of magnetic phases and the piezoelectric volume fraction, v . Using the most suitable piezoelectric and magnetic phases and optimized thickness for the components are the avenues for increasing the ME coupling in the layered structures based on the piezoelectric bimorph and magnetostrictive component.

RESULTS AND DISCUSSION

The following material parameters (in SI units) are used for estimates: ${}^p d_{31} = -175 \times 10^{-12}$ m/V, ${}^p \epsilon_{33}/\epsilon_0 = 1750$; ${}^p s_{11} = 15.3 \times 10^{-12}$ m²/N; ${}^m q_{11} = 1.25 \times 10^{-9}$ m/A; ${}^m s_{11} = 10 \times 10^{-12}$ m²/N. The piezomagnetic coefficient is determined from magnetostriction λ_1 versus bias magnetic field curve (Fig. 2) as $\partial\lambda_1/\partial H$. For increasing H_{dc} , ${}^m q_{11}$ shows a rapid rise to a peak value for $H_{dc} \approx 12$ Oe. However, the bias field of 30 Oe is used in this study due to limitations of the measuring technique for ME characterization.

Figure 3 shows the estimated PZT volume fraction dependence of the ME voltage coefficient for layered structures of PZT bimorph/Metglas and PZT/Metglas bilayer. The ME voltage coefficient

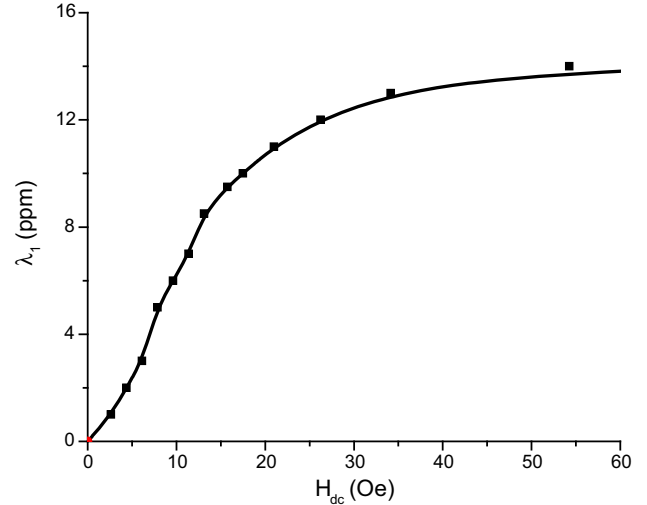


Fig. 2. Data on magnetostriction of Metglas versus bias magnetic field.

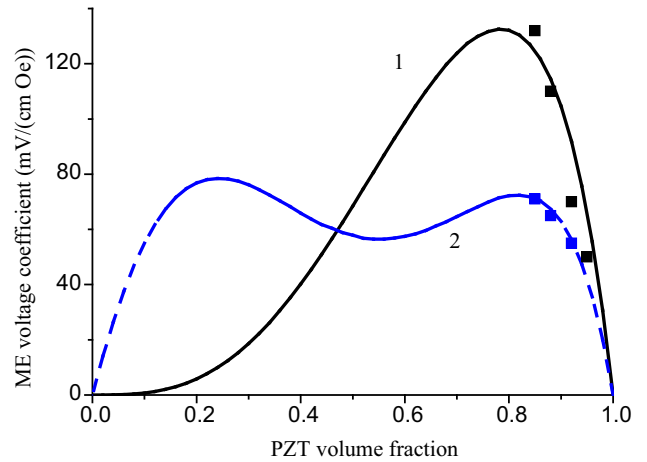


Fig. 3. PZT volume fraction dependence of ME voltage coefficient for the layered structure of PZT bimorph/Metglas (1) calculated according to Eq. 4, and the PZT/Metglas bilayer (2) calculated according to Eq. 5. Solid lines and dots correspond to estimates and data, respectively. Data are obtained for 1–4 layers of Metglas.

versus PZT volume fraction for PZT/Metglas bilayer is estimated by using the expression²:

$$\alpha_{E31} = \frac{(1-v)v^m q_{11} p d_{31} [(m s_{11} - p s_{11})v^3 + p s_{11}(3v^2 - 3v + 1)]}{2\{(m s_{11} - p s_{11})v[(m s_{11} - p s_{11})v^3 + 4^p s_{11}(v^2 + 1) - 6^p s_{11}v] + p s_{11}^2\} p \epsilon_{33}} \quad (5)$$

One observes a satisfactory agreement between theory and data in Fig. 3. It should be noted that, contrary to expectation, the presented rough model gives underestimated values of the ME voltage coefficient compared with the experimental data. This can be accounted for by an essential error in determining the piezomagnetic coefficient based on data in Fig. 2. The error of computation of this coefficient is estimated at approximately 10%.

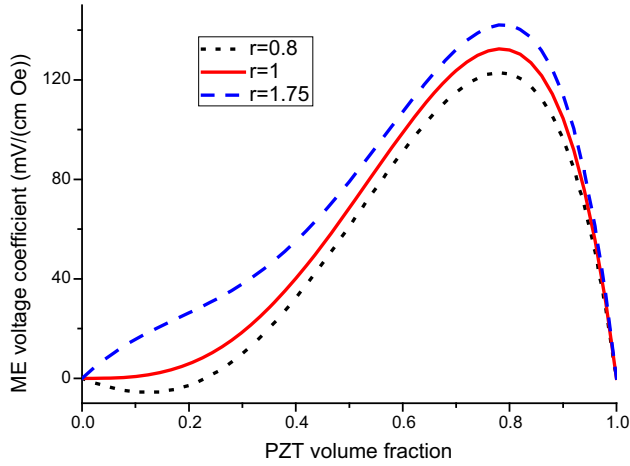


Fig. 4. Estimated PZT volume fraction dependence of the ME voltage coefficient for a layered structure of PZT/PZT/Metglas with opposite poling directions of PZT layers at different thickness ratios, $r = p^1 t / p^2 t$ ($p^1 t$ and $p^2 t$ are the thicknesses of the upper and lower PZT layers). Equation 6 was used for the calculations.

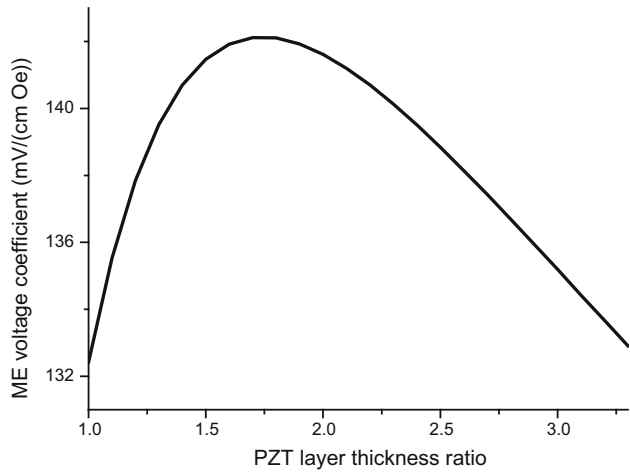


Fig. 5. Estimated dependence of the ME voltage coefficient on the thickness ratio $r = p^1 t / p^2 t$ for a layered structure of PZT/PZT/Metglas with opposite poling directions of PZT layers at $v = 0.79$. Equation 6 is used for calculations.

The piezoelectric bimorph-based structure leads to a maximum in $\alpha_{E,31}$ at a higher value of v compared to the piezoelectric/magnetostrictive bilayer. The ME coefficient is found to be approximately two times larger than for the traditional PZT/Metglas bilayer. The reason for this is as follows. The strain in both piezoelectric layers is a sum of the axial and flexural Z-dependent strains. For the traditional PZT/Metglas bilayer, the flexural stresses in the lower and upper halves of the piezoelectric layer are opposite in sign and the total average stress in the piezoelectric layer decreases due to bending. Note that average stress determines the ME output. In contrast to this, the stresses in the piezoelectric layers of the PZT bimorph/Metglas structure change their sign simultaneously with the

change in poling direction, which is possible at appropriate PZT and Metglas volume fractions. The signs of the induced voltage in both layers appear equal and the total ME output increases.

Replacing the PZT bimorph by two PZT layers with different thickness can increase the ME output. To find the optimized PZT layer thickness ratio, we considered the structure which includes two PZT layers with different thicknesses and opposite poling directions (Fig. 1). Similarly to the calculation of ME coupling in the PZT bimorph-based structure, one can obtain an expression for the output voltage:

$$\alpha_{E,31} = -\frac{p d_{31}}{t H_1^p \epsilon_{33}} \left(\int_{-p^1 t/2}^{p^1 t/2} p^1 T_1 dz + \int_{-p^2 t/2}^{p^2 t/2} p^2 T_1 dz \right). \quad (6)$$

In this expression, the stress components can be found from Eqs. 2 and 3 taking into account Eq. 1.

The PZT volume fraction dependence of the ME voltage coefficient is shown in Fig. 4 for layered structures of PZT/PZT/Metglas at different thickness ratios, $r = p^1 t / p^2 t$, with $p^1 t$ and $p^2 t$ being the thicknesses of upper and lower PZT layer (Fig. 1). Figure 5 shows the estimated dependence of ME voltage coefficient on thickness ratio r for layered structure of PZT/PZT/Metglas. The total PZT thickness related to the PZT volume fraction v that equals the PZT to sample thickness ratio.

Figures 4 and 5 show that the PZT layer thickness ratio of 1–3 results in a slight increase in ME coupling strength for a PZT/PZT/Metglas structure compared to a PZT bimorph/Metglas structure. The peak value of the obtained increase was about 8% for $r = 1.75$.

In summary, we have investigated the ME coefficient in layered structures of a PZT bimorph and magnetostrictive Metglas. The ME coefficient in this structure was found to be approximately two times larger than in the traditional PZT/Metglas bilayer. The observed enhancement in ME coupling strength is related to equal signs of induced voltage in both PZT layers, with opposite poling directions due to the flexural deformations. The flexural deformations distribution provides an increase in induced voltage at specified PZT volume fractions. This investigation promises potential for sensor and technological applications.

ACKNOWLEDGEMENT

The research was supported by a grant from the Russian Science Foundation (Grant No: 15-19-10036).

REFERENCES

1. N.A. Spaldin and M. Fiebig, *Science* 309, 391 (2005).
2. M.I. Bichurin and V.M. Petrov, *Modeling of Magnetolectric Effects in Composites. Springer Series in Materials Science*, Book 201, (Dordrecht: Springer, 2014).

3. C.-W. Nan, M.I. Bichurin, C. Dong, D. Viehland, and G. Srinivasan, *J. Appl. Phys.* 103, 031101 (2008).
4. M. Fiebig, *J. Phys. D* 38, R123 (2005).
5. V.M. Petrov and G. Srinivasan, *Phys. Rev. B* 78, 184421 (2008).
6. A.A. Bush, K.E. Kamentsev, V.F. Mesherykov, Y.K. Fetisov, D.V. Chashin, and L.Y. Fetisov, *Tech. Phys.* 54, 1314 (2009).
7. J. Zhai, Z. Xing, S. Dong, J. Li, and D. Viehland, *J. Am. Ceram. Soc.* 91, 351 (2008).
8. S. Zhong, S.P. Alpay, M.W. Cole, E. Ngo, S. Hirsch, and J.D. Demaree, *Appl. Phys. Lett.* 90, 092901 (2007).
9. S. Ueda, *J. Therm. Stress.* 27, 291 (2004).
10. J.L. Sun, Z.G. Zhou, and B. Wang, *Acta Mech. Sin.* 37, 9 (2005).
11. C. Sudakar, R. Naik, G. Lawes, J.V. Mantese, A.L. Micheli, G. Srinivasan, and S.P. Alpay, *Appl. Phys. Lett.* 90, 062502 (2007).
12. S.P. Timoshenko and D.H. Young, *Vibration Problems in Engineering* (New York: Van Nostrand, 1995).